Effects of energy offsets and molecular packing on exciton and charge carrier dynamics in small-molecule donor-acceptor composites

Keshab Paudel[a], Brian Johnson[a], Afina Neunzert[a], Mattson Thieme[a] , John Anthony[b] and Oksana Ostroverkhova[a]

[a]Oregon State University, Corvallis, Oregon 97331, U.S.A.
[b]University of Kentucky, Lexington, Kentucky 40506, U.S.A.

ABSTRACT

We present a study of optical, photoluminescent (PL), and photoconductive properties of small-molecule D/A bulk heterojunctions of functionalized fluorinated anthradithiophene (ADT-R-F) and pentacene (Pn-R-F8) derivatives. We chose one of the ADT derivatives, ADT-TES-F, which exhibits a 2D "brick-work" π-stacking, as the donor, and ADT-TIPS-F (2D "brick-work"), ADT-TSBS-F (1D "sandwich-herringbone"), Pn-TIPS-F8 (2D "brick-work"), or Pn-TCHS-F8 (1D "sandwich-herringbone"), as acceptors. We measured PL and photoconductivity at time scales from sub-nanoseconds to many seconds after photoexcitation, at various acceptor concentrations, under various experimental conditions. The choice of acceptors enabled us to distinguish between effects of the LUMO energy offsets between the donor and acceptor molecules and those of the molecular packing in the acceptor domains on exciton and charge carrier dynamics.

Keywords: organic semiconductors, bulk heterojunctions, organic donor-acceptor materials, photoconductivity, exciplex

1. INTRODUCTION

Understanding of exciton and charge carrier dynamics in organic donor-acceptor (D/A) heterojunctions is crucial for the development of organic solar cells, light-emitting diodes, and photorefractive applications. Thus far, most effort has been directed towards studies of D/A materials with polymer donors and fullerene acceptors, while small-molecule D/A bulk heterojunctions (SMBHJ) remained relatively unexplored. Several functionalized anthradithiophene (ADT) and pentacene (Pn) derivatives exhibited high charge carrier mobilities,[1,2] fast photoresponse,[3] high photoconductive gains,[4] and strong PL.[4,5] For example, hole mobilities of over 1.5 cm^2/Vs have been reported in solution-processed films of Pn functionalized with triisopropylsilylethynyl (TIPS) groups (Pn-TIPS) and fluorinated ADT functionalized with triethylsilylethynyl (TES) side groups (ADT-TES-F).[1,6] Our effort has been focused on high performance solution processable small molecule D/A bulk heterojunctions consisting of functionalized derivatives of fluorinated ADT (ADT-R-F) and Pn (Pn-R-F8), where R represents the side groups (Fig.1). In this paper, we present optical, PL, and (photo)conductive properties of SMBHJs based on several combinations of ADT and Pn derivatives. In particular, we sought to separately study effects of the LUMO energy offsets between the donor and acceptor molecules and of molecular packing in the film on exciton and charge carrier dynamics.

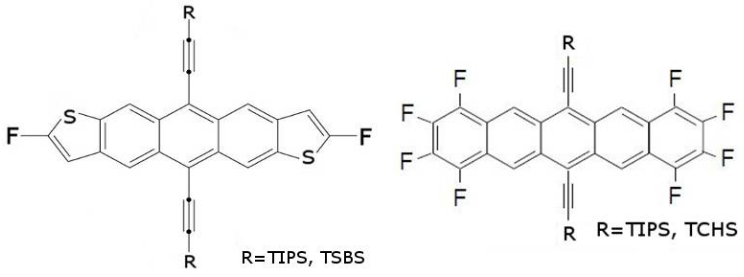

Figure 1. Chemical structures of ADT-R-F derivatives (left) and Pn-R-F8 derivatives (right) used in our studies.

2. EXPERIMENTAL

2.1 Materials

For our studies, we chose ADT-TES-F as the donor and either other ADT-R-F derivatives (R = TIPS or TSBS, where TSBS = tri-sec-butylsilylethynyl) or Pn-R-F8 (R = TIPS or TCHS, where TCHS = tricyclohexylsilylethynyl) derivatives as acceptors. The choice of the acceptors was motivated by the following considerations. It has been shown that the side groups R do not significantly affect molecular properties including HOMO and LUMO energies,[4,7] while considerably impacting molecular packing in the solid state. Thus, we expect that most effects of introducing an ADT-R-F acceptor to the ADT-TES-F donor would be due to molecular packing. This is in constrast to ADT-TES-F/Pn-R-F8 D/A composites which, in addition to molecular packing effects, would also incorporate effects of the LUMO differences between the ADT-TES-F donor and Pn-R-F8 acceptor. The HOMO (LUMO) energies of the ADT-R-F and Pn-R-F8 derivatives were 5.35 eV (3.05 eV) and 5.55 eV (3.6 eV), respectively.[7] The choice of the side groups R in our acceptors was governed by particular packing motifs we sought to explore in our SMBHJs. In particular, both ADT and Pn acceptors with TIPS side groups are known to exhibit a 2D "brick-work" π-stacking motif, similar to that of the ADT-TES-F donor.[8] In contrast, ADT-TSBS-F and Pn-TCHS-F8 pack in the 1D "sandwich-herringbone" structures, which have been reported to be favorable for an organic solar cell performance.[9] In addition, TIPS, TSBS, and TCHS side groups have considerably different volumes (TIPS $<$TSBS $<$TCHS),[7,10] which causes differences in the D/A separation at the D/A interface, depending on the R.

2.2 Sample preparation

To prepare thin D/A films, 30 mM solutions containing ADT-TES-F donor and ADT-TIPS-F, ADT-TSBS-F, Pn-TIPS-F8 or Pn-TCHS-F8 acceptor mixed at appropirate concentrations in chlorobenzene were used. For each D/A combination, solutions with 98/2, 95/5, 93/7 and 90/10 weight percentages (% wt/wt) of D/A were prepared and 10 μL solutions of each mixture were spun at 3000 rpm on a glass substrate having 10 pairs of photolithographically deposited Cr/Au (5 nm/50 nm thick) interdigitated electrodes, 1 mm long and 25μm wide fingers, with a gap of 25μm between fingers of opposite electrodes. Each substrate was pre-treated with a pentafluorobenzenethiol (PFBT) in order to form a self-assembled monolayer,[11] which was found to facilitate crystallization in both the ADT and Pn derivatives and reduce the injection barrier on gold by lowering its work function.[12] Film samples for the pristine materials were also prepared using the same protocol. Such preparation method yielded polycrystalline films, as confirmed by x-ray diffraction[6] and optical imaging.

2.3 Optical absorption and PL measurements

Optical absorption spectra were taken with an Ocean Optics USB4000 spectrometer by transmitting light from an Ocean Optics LS-1 tungsten halogen lamp through the film samples. PL was excited by a 532 nm continuous wave (cw) light from a frequency doubled $Nd:YVO_4$ laser from Coherent, Inc. PL spectra were then collected using Ocean Optics USB2000 spectrometer in a 45° reflection geometery, through a 535 LP filter.
Time-resolved PL was excited with 355 nm, 500 ps, 44.6kHz, Q-switched, frequency-tripled Nd:YAG laser from Nanolase, Inc. Signals were acquired by a time-correlated singal-photon counter (TCSPC) board (Pico-Quant Time Harp 200) through a single-photon avalanche photodiode (SPAD) from Micro Photon Devices.[4] In ADT-TES-F/Pn-R-F8 composites, transient PL data were collected separately from the ADT-TES-F PL region (selected by the 650SP filter) and exciplex (charge transfer exciton) PL region (selected by the 680LP filter) of the PL spectrum. The instrument response function (IRF) was recorded by using scattered light by an aluminum-coated glass slide. The time resolution was about 500 ps, limited by the laser pulse width. For electric field-dependent PL measurements, voltage was applied using a Keithley 237 source-measure unit. The field strength, E, was calculated by using $E = V/L$ where L is the gap between the opposite electrodes.

2.4 Photocurrent Measurements

Continuous wave (cw) photocurrents were excited with a 532 nm (frequency-doubled Nd:YVO_4) or 633 nm (HeNe) laser incident from the substrate side of the thin-film samples. Current-voltage (I-V) measurements in the dark and under photoexcitation were taken using a Keithley 237 source-measure unit. Photocurrents were then calculated by subtracting dark currents from the corresponding currents under illumination. In order to observe the long time scale cw photocurrent dynamics, the voltage was applied and, after the dark current have stabilized, the incident laser beam was turned on for about 80 s and then turned off using a Thorlabs SH05 shutter, and the photocurrent rise and decay dynamics were recorded with

the Keithley 237 source-measure unit.

Transient photocurrents were excited by the 355 nm 500 ps pulsed laser described above incident on the substrate side of the sample. The Keithley 237 source-measure unit provided the bias voltage, and photocurrent signals, preamplified by a Centellax UAOL6032VM broadband amplifier, were collected by a 50GHz digital sampling oscilloscope (DSO) (CSA8200/Tektronix 80E01). Resolution of the set up was ~0.5 ns, limited by the laser pulse width. All the experimental data were collected at room temperature.

3. RESULTS AND DISCUSSION

3.1 Optical and PL properties

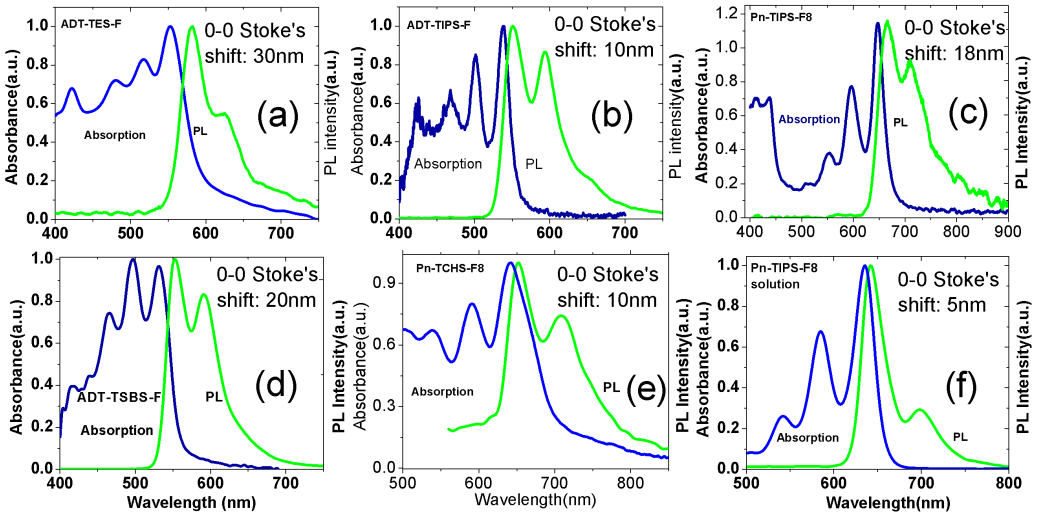

Figure 2. (a)-(e) Absorption and PL spectra of the pristine films of ADT-TES-F, ADT-TIPS-F, Pn-TIPS-F8, ADT-TSBS-F and Pn-TCHS-F8, respectively. (f) Absorption and PL spectra of Pn-TIPS-F8 in solution.

Optical absorption and PL spectra of the pristine film samples of all derivatives used in this study are shown in Fig. 2(a)-(e), which highlights effects of molecular packing on the optical and PL properties of films. All spectra exhibit the Frank-Condon progression of vibronic peaks, where the prominent ones correspond to the 0-0 and 0-1 transitions. In solution, all ADT-R-F (Pn-R-F8) derivatives have similar absorption and PL spectra, independent of R groups, with an absorption and PL maxima occurring at, for example, 528 nm (635 nm) and 536 nm (642 nm) in toluene (chlorobenzene) (Fig.2(f)).[4] Optical absorption of films exhibits a red-shift with respect to that of solutions (Fig.2),[5] which has been attributed to the enhanced Coulomb interaction of the molecules with their surrounding and exchange interaction between translationally equivalent molecules in films.[13] The amount of this red shift is determined by molecular packing in the film and depends on the strength of intermolecular interactions. Since the main backbone structures of all three ADT-R-F derivatives and of two Pn-R-F8 derivatives are same (Fig.1), the observed differences in the spectra are due to the variations in crystallinity and packing, dictated by the choice of the side group substituents R. For example, the molecular packing in the ADT-TES-F film is such that intermolecular interactions are strongest of all ADT-R-F derivatives, followed by the ADT-TIPS-F and ADT-TSBS-F (lowest-energy film absorption peaks at 552 nm, 538 nm, and 532 nm, respectively, as compared to that at 528 nm in solution). Low red shifts in absorption spectra of pristine films of both Pn-R-F8 derivatives (Fig. 2(c),(e),(f)) suggest weak intermolecular interactions in these films. For both ADT and Pn derivatives, the intermolecular interactions were weaker in films of derivatives that pack in the 1D "sandwich-herringbone" structure, as compared to 2D "brick-work" structure. Molecular packing-dependent differences in the Stoke's shifts (included in Fig. 2) were also observed and were larger in films as compared to solutions.[4,5]

Optical absorption of films of all D/A composites studied was dominated by that of the ADT-TES-F donor (Fig. 2(a)). PL spectra and lifetimes of D/A composites enable differentiation between charge and energy transfer and observation of the changes in exciton dynamics upon acceptor addition, depending on the acceptor.[7,14] The steady-state PL spectra of

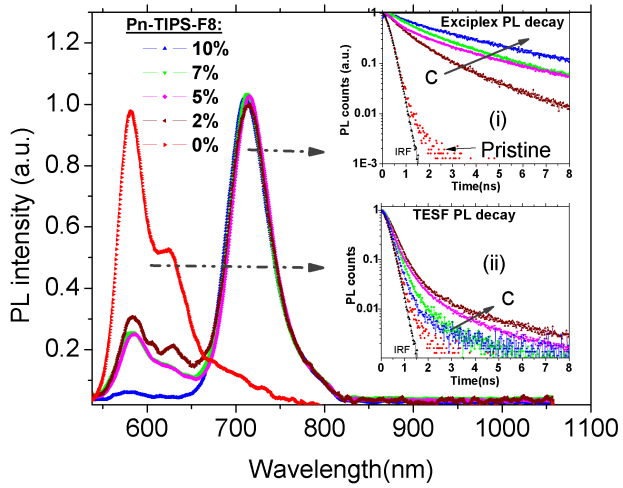

Figure 3. PL spectra of ADT-TES-F/Pn-TIPS-F8 composite films at various Pn-TIPS-F8 concentrations. Insets show the corresponding transient PL data acquired separately for (i) exciplex emission and (ii) ADT-TES-F emission regions of the PL spectra. PL decay from a pristine ADT-TES-F film and IRF are also included. As the acceptor concentration (C) increases, the PL decays become slower.

all ADT-TES-F/ADT-R-F composites studied were dominated by the ADT-TES-F donor emission (Fig.2(a)); however, the PL lifetimes increased as the concentration an ADT-R-F as acceptor is increased,[10] due to the disruption of ADT-TES-F crystalline domains, which effectively limited delocalization of the ADT-TES-F exciton that, in turn, reduced the non-radiative recombination.[5] In addition to the change in PL lifetimes, the ADT-TES-F domain disruption led to the increase in the PL intensity from ADT-TES-F/ADT-R-F films upon an increase in the ADT-R-F concentration. The effect was more pronounced in the composites with the ADT-TSBS-F acceptor, as compared to ADT-TIPS-F, which suggests that 1D "sandwich-herringbone" packing of the ADT-TSBS-F is more disruptive to the packing of the ADT-TES-F donor, as compared to 2D "brick-work" packing of ADT-TIPS-F. In ADT-TES-F/Pn-R-F8 films, in which the LUMO offset between the ADT-TES-F donor and Pn-R-F8 acceptor was about 0.55 eV, exciplex formation as a result of partial charge transfer between ADT-TES-F and Pn-R-F8 was observed.[7,14] Figure 3 shows steady-state PL spectra for ADT-TES-F/Pn-TIPS-F8 composite films at various Pn-TIPS-F8 concentrations. As the acceptor concentration increased, PL of the ADT-TES-F donor (peaked at ~585 nm) was efficiently quenched, while that of the exciplex (peaked at ~ 715nm) increased. At 10% Pn-TIPS-F8 concentration, the PL from the ADT-TES-F donor constituted only about ~ 2% of the total PL emission in this composite. The redistribution of PL intensity between the ADT-TES-F donor and the exciplex was accompanied by changes in the PL lifetimes (inset of Fig.3). The PL decay in the spectral region of >680 nm was longer as the acceptor concentration increased (inset (i)), due to the exciplex emission, characterized by longer lifetimes[7] dominating the PL at these wavelengths. A similar effect was observed at wavelengths below 650 nm (inset (ii)), at which emission from the ADT-TES-F donor dominated at low acceptor concentrations, but was overcome by the tail of the exciplex emission at higher acceptor concentrations. Qualitatively, similar effects were observed in ADT-TES-F/Pn-TCHS-F8 films. However, a shorter PL exciplex lifetime and much weaker quenching of the ADT-TES-F donor PL as a function of Pn-TCHS-F8 concentration were observed. The former suggests a more dissociative (less tightly bound) ADT-TES-F/Pn-TCHS-F8 exciplex due to a considerably larger D/A separation in these composites, caused by a bulky TCHS group, as compared to that in ADT-TES-F/Pn-TIPS-F8 composites.[7] The latter indicates a less efficient charge transfer between ADT-TES-F and Pn-TCHS-F8 as compared to that between ADT-TES-F and Pn-TIPS-F8, partially attributed to differences in the D/A interfacial area caused by the 1D packing of Pn-TCHS-F8 as compared to the 2D packing of Pn-TIPS-F8.[10]

3.2 Photoconductive properties

3.2.1 Transient photocurrent

Transient photocurrents obtained under a 500 ps pulsed excitation of a pristine ADT-TES-F film and ADT-TES-F/ADT-TIPS-F composites at several acceptor concentrations measured at the applied voltage of 100 V are shown in Fig.4(a); voltage dependences of peak photocurrent for a pristine ADT-TES-F film and ADT-TES-F/Pn-TCHS-F8 composites at

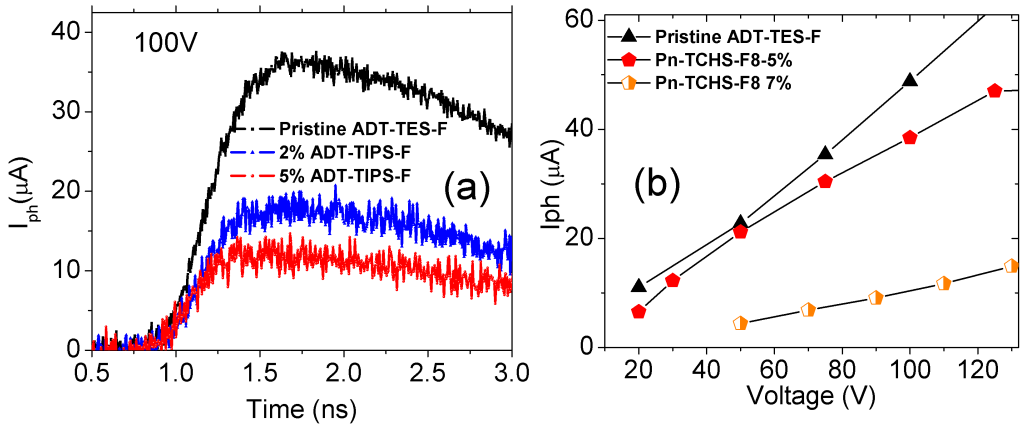

Figure 4. (a) Transient photocurrents obtained in a pristine ADT-TES-F film and ADT-TES-F/ADT-TIPS-F 2% and ADT-TES-F/ADT-TIPS-F 5% composites at 100 V. (b) Peak transient photocurrent as a function of applied voltage in a pristine ADT-TES-F film and ADT-TES-F/Pn-TCHS-F8 composites at 5% and 7% acceptor concentration.

several concentrations are shown in Fig.4(b). At all values of applied voltage, photocurrents for the D/A composite samples were lower than that for the pristine ADT-TES-F film, for either ADT-R-F or Pn-R-F8 acceptors (Fig.4), and no transient photocurrents could be observed in any D/A composite with the acceptor concentration of 10%. In all samples, the photocurrent rise time was limited by the laser pulse width, and the exact dynamics was dependent upon the D/A separation at the D/A interface.[7] At low acceptor concentrations, D/A composites with the Pn-F8-R acceptors exhibited higher photocurrent amplitudes than ADT-TES-F/ADT-R-F composites, due to the contribution of exciplex dissociation to the charge generation.[5,14] At higher acceptor concentrations, however, photocurrent in composites with either Pn-R-F8 or ADT-R-F acceptors were low, regardless of the packing motif of the acceptor, which suggests that the exciplex dissociation into free carriers was inefficient, as expected from highly emissive exciplexes observed in ADT-TES-F/Pn-R-F8 composites (Fig.3), and it did not compensate for a decrease in charge carrier mobility due to the disruption of ADT-TES-F domain crystallinity upon an introduction of the acceptor.

3.2.2 Dark currents and cw photocurrents

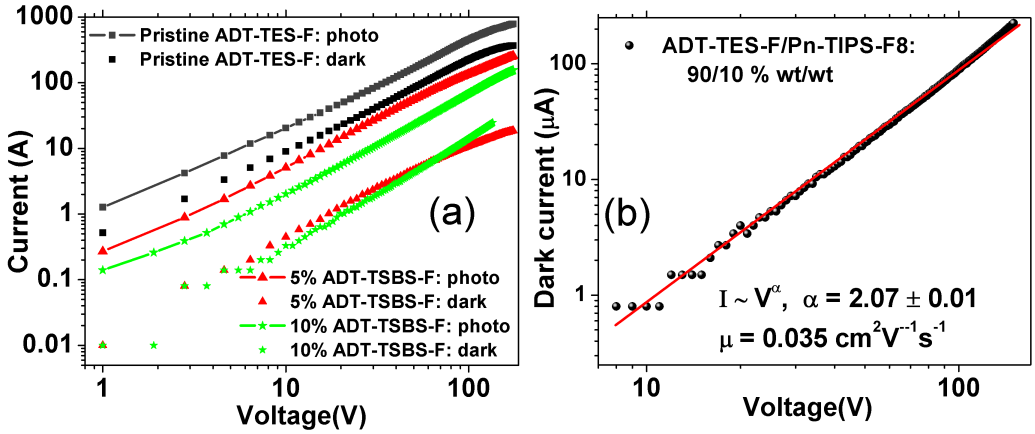

Figure 5. (a) Dark currents and cw photocurrents obtained under a 532 nm 400 μW excitation of a pristine ADT-TES-F film and ADT-TES-F/ADT-TSBS-F composites at several concentrations. (b) Dark current for a ADT-TES-F/Pn-TIPS-F8 10% film exhibiting SCLC behavior.

An example of dark currents and cw photocurrents obtained at 532 nm, 400 μW illumination, at various applied voltages, in a pristine ADT-TES-F film and ADT-TES-F/ADT-TSBS-F composites at 5% and 10% concentration of ADT-

TSBS-F is shown in Fig.5(a). Space charge limited currents (SCLCs), characterized by current (I)-voltage (V) dependence in the form of $I \sim V^2$ (Fig.5(b)) and indicative of efficient hole injection from the Au electrodes, could be observed in several samples. In our planar electrode geometry, where the current flows along a layer of unknown thickness, there is no analytical current-voltage relationship.[15,16] In the infinitely thin film approximation, justified by our spin-coated film thickness (d) being much lower than the electrode gap (L) of 25 μm,

$$j = \frac{2\mu_{eff}\varepsilon\varepsilon_0 V^2}{\pi L^2} \quad (1)$$

where j is the linear current density, ε is the relative dielectric constant, and ε_0 is the permitivitty of free space. Using the dark currents, SCLC effective mobilities ($\mu_{eff} = \mu\theta$, where θ is the ratio of free to trapped charge carriers) were calculated using Eq. 1 and yielded 0.035-0.04 $cm^2/(Vs)$, depending on the sample (Fig.5(b)). These should be considered to be lower bounds on hole mobilities in our films, as the trap-limited regime has not been achieved in any of the films.

In most samples, photocurrents at 532 nm 400 μW excitation were considerably higher than dark currents (Fig.5(a)). However, as the acceptor concentration increased, the photocurrents decreased in all composites, so that at 10% acceptor concentrations, the photocurrents were at least a factor of $\sim$2 lower than those in pristine ADT-TES-F films under similar conditions. Photocurrents could also be observed under a 633 nm excitation; however, excitation powers of at least 2.5 mW were needed to achieve good signal-to-noise ratio due to low absorption at this wavelength.

Figure 6 illustrates differences in cw photocurrent dynamics at (a) 532 nm and (b) 633 nm 2.5 mW photoexcitation,

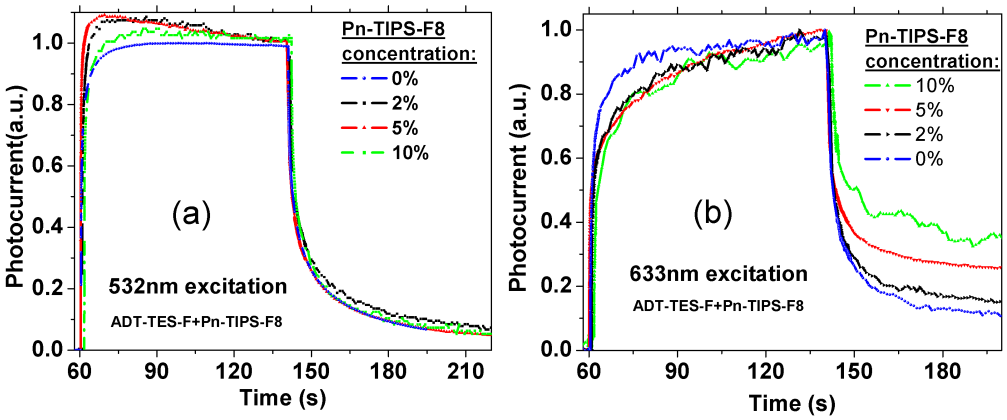

Figure 6. Cw photocurrent dynamics of ADT-TES-F/Pn-TIPS-F8 films at various acceptor concentrations at (a) 532 nm excitation (b) 633 nm excitation at 2.5 mW at the applied voltage of 50 V. Light was turned on at 62 s and turned off at 140 s. Photocurrents were normalized by their values at time t = 140 s.

in the ADT-TES-F/Pn-TIPS-F8 composites at various concentrations. Strong absorption of the 532 nm light leads to efficient charge photogeneration, followed by bimolecular recombination, which manifests through the slow decay of the photocurrent under illumination. Under these conditions, the cw photocurrent decay dynamics in these composites after the light was turned off did not depend on the acceptor concentration and was similar to that in the pristine ADT-TES-F films, which suggests that the long-time-scale charge carrier detrapping and recombination properties in these composites are dominated by those of the ADT-TES-F donor.[7] In contrast, the decay dynamics of the photocurrent under 633 nm excitation became slower as the acceptor concentration increased. Based on the optical absorption properties of these films, absorption at this excitation wavelength is dominated by that of defect states in the ADT-TES-F donor domains. As a result, the photocurrent amplitudes at this wavelength were at least an order of magnitude lower than those at 532 nm at same light intensity and applied voltage, and the photocurrent dynamics was especially sensitive to defects. As the acceptor concentration increased, the ADT-TES-F donor domains were increasingly disrputed, leading to larger trap densities and deeper traps which changed the photocurrent dynamics.

4. CONCLUSIONS

We examined effects of the LUMO energy offset between the donor and acceptor and of molecular packing on the photoluminescent and photoconductive properties of small-molecule D/A composites with acceptor concentrations up to 10%. In ADT-TES-F/ADT-R-F composites, in which the LUMO energy offset was minimal, the PL was dominated by that of the ADT-TES-F donor, and the PL properties of the ADT-TES-F exciton changed as the acceptor concentration increased due to the disruption of the ADT-TES-F crystalline domain structure. A larger change was observed in the composites with the ADT-TSBS-F acceptor, as compared to those with the ADT-TIPS-F acceptor, which we attribute to a more disruptive 1D "sandwich-herringbone" packing of the ADT-TSBS-F in contrast to 2D "brick-work" packing of the ADT-TIPS-F that is similar to that of the ADT-TES-F donor. In ADT-TES-F/Pn-R-F8 composites, in which the D/A LUMO offset was ~0.55 eV, exciplex formation was observed. The PL of the ADT-TES-F donor was almost entirely quenched in the D/A composite with 10% of Pn-TIPS-F8, which suggests that the 2D packing of this acceptor promotes a large D/A interfacial area; the quenching was less efficient in composites with Pn-TCHS-F8 acceptor that exhibits the 1D packing.

In all D/A composites, the photocurrents were reduced as compared to those in pristine ADT-TES-F donor films, most likely due to a reduced charge carrier mobility caused by disruption of ADT-TES-F crystallinity. At low acceptor concentrations, photocurrents in ADT-TES-F/Pn-R-F8 composites were higher than those in the ADT-TES-F/ADT-R-F composites, due to the contribution of exciplex dissociation to charge carrier photogeneration. At higher acceptor concentrations, the photocurrents were low in both ADT-TES-F/ADT-R-F and ADT-TES-F/Pn-R-F8 composites, regardless of the packing motif, due to a dominant effect of a structural disruption in the ADT-TES-F donor domains, detrimental for charge carrier mobility. At ns time scales, the photocurrent dynamics in D/A composites depended upon the D/A separation at the D/A interfaces. At longer time scales of many tens of seconds, effects of changes in charge trapping properties upon the acceptor concentration increase were observed in the cw photocurrent dynamics.

Acknowledgements

We thank J. Ward and Prof. O. D. Jurchescu for helpful suggestions regarding the PFBT treatment of the substrates. This work was supported by the NSF grant DMR-1207309.

REFERENCES

1. S. K. Park, D. A. Mourey, S. Subramanian, J. E. Anthony, and T. N. Jackson, "High-mobility spin-cast organic thin film transistors," *Applied Physics Letters* **93**(4), p. 043301, 2008.
2. S. K. Park, T. N. Jackson, J. E. Anthony, and D. A. Mourey, "High mobility solution processed 6,13-bis(triisopropylsilylethynyl) pentacene organic thin film transistors," *Applied Physics Letters* **91**(6), p. 063514, 2007.
3. J. Day, S. Subramanian, J. E. Anthony, Z. Lu, R. J. Twieg, and O. Ostroverkhova, "Photoconductivity in organic thin films: From picoseconds to seconds after excitation," *Journal of Applied Physics* **103**(12), p. 123715, 2008.
4. A. D. Platt, J. Day, S. Subramanian, J. E. Anthony, and O. Ostroverkhova, "Optical, fluorescent, and (photo)conductive properties of high-performance functionalized pentacene and anthradithiophene derivatives," *The Journal of Physical Chemistry C* **113**(31), pp. 14006–14014, 2009.
5. A. D. Platt, M. J. Kendrick, M. Loth, J. E. Anthony, and O. Ostroverkhova, "Temperature dependence of exciton and charge carrier dynamics in organic thin films," *Phys. Rev. B* **84**, p. 235209, Dec 2011.
6. D. J. Gundlach, J. E. Royer, S. K. Park, S. Subramanian, O. D. Jurchescu, B. H. Hamadani, a. J. Moad, R. J. Kline, L. C. Teague, O. Kirillov, C. a. Richter, J. G. Kushmerick, L. J. Richter, S. R. Parkin, T. N. Jackson, and J. E. Anthony, "Contact-induced crystallinity for high-performance soluble acene-based transistors and circuits.," *Nature materials* **7**, pp. 216–21, Mar. 2008.
7. M. J. Kendrick, A. Neunzert, M. M. Payne, B. Purushothaman, B. D. Rose, J. E. Anthony, M. M. Haley, and O. Ostroverkhova, "Formation of the donoracceptor charge-transfer exciton and its contribution to charge photogeneration and recombination in small-molecule bulk heterojunctions," *The Journal of Physical Chemistry C* **116**(34), pp. 18108–18116, 2012.
8. J. E. Anthony, "Functionalized acenes and heteroacenes for organic electronics," *Chemical Reviews* **106**(12), pp. 5028–5048, 2006.
9. Y.-F. Lim, Y. Shu, S. R. Parkin, J. E. Anthony, and G. G. Malliaras, "Soluble n-type pentacene derivatives as novel acceptors for organic solar cells," *J. Mater. Chem.* **19**, pp. 3049–3056, 2009.

10. K. Paudel, B. Johnson, A. Neunzert, M. Thieme, J. Anthony, and O. Ostroverkhova, "In preparation," *Journal of Physical Chemistry C* **x**, 2013.
11. J. W. Ward, M. a. Loth, R. J. Kline, M. Coll, C. Ocal, J. E. Anthony, and O. D. Jurchescu, "Tailored interfaces for self-patterning organic thin-film transistors," *Journal of Materials Chemistry* **22**(36), p. 19047, 2012.
12. C. H. Kim, H. Hlaing, F. Carta, Y. Bonnassieux, G. Horowitz, and I. Kymissis, "Templating and charge injection from copper electrodes into solution-processed organic field-effect transistors," *ACS Applied Materials & Interfaces* **5**(9), pp. 3716–3721, 2013.
13. M. Pope and C. Swenberg, *Electronic processes in organic crystals and polymers*, Monographs on the physics and chemistry of materials, Oxford University Press, 1999.
14. W. E. B. Shepherd, A. D. Platt, M. J. Kendrick, M. A. Loth, J. E. Anthony, and O. Ostroverkhova, "Energy transfer and exciplex formation and their impact on exciton and charge carrier dynamics in organic films," *The Journal of Physical Chemistry Letters* **2**(5), pp. 362–366, 2011.
15. J. Day, A. D. Platt, S. Subramanian, J. E. Anthony, and O. Ostroverkhova, "Influence of organic semiconductor-metal interfaces on the photoresponse of functionalized anthradithiophene thin films," *Journal of Applied Physics* **105**(10), p. 103703, 2009.
16. W. Hu, B. Gompf, J. Pflaum, D. Schweitzer, and M. Dressel, "Transport properties of [2,2]-paracyclophane thin films," *Applied Physics Letters* **84**(23), pp. 4720–4722, 2004.